# *SWELL1* is a glucose sensor required for β-cell excitability and insulin secretion

Chen Kang[1], Susheel K. Gunasekar[1], Anil Mishra[1], Litao Xie[1], Yanhui Zhang[1], Saachi Pai[1], Yiwen Gao[1], Andrew W. Norris[2,3], Samuel B. Stephens[1,3], Rajan Sah[1,3,4]

[1]Department of Internal Medicine, Division of Cardiovascular Medicine, University of Iowa, Carver College of Medicine, Iowa City, IA, 52242

[2]Department of Pediatrics, University of Iowa, Carver College of Medicine, Iowa City, IA, 52242

[3]Fraternal Order of the Eagles Diabetes Research Center, Iowa City, IA, 52242

[4]Abboud Cardiovascular Research Center, University of Iowa, Carver College of Medicine, Iowa City, IA, 52242

*** Corresponding Author:**
**Dr. Rajan Sah**
**169 Newton Rd. PBDB 4334**
**Iowa City, Iowa 52242**
**Phone: 319-353-5660 Email: rajan-sah@uiowa.edu**

**Abstract**

Insulin secretion from the pancreatic β-cell is initiated by activation of voltage-gated $Ca^{2+}$ channels (VGCC) to trigger $Ca^{2+}$-mediated insulin vesicle fusion with the β-cell plasma membrane. The firing of VGCC depends on the β-cell membrane potential, which is in turn mediated by the balance of depolarizing (excitatory) and hyperpolarizing (inhibitory) ionic currents[1-3]. While much attention has focused on inhibitory potassium currents[4-10] there is little knowledge about the excitatory currents required to depolarize the β-cell, including the molecular identity of these excitatory currents[3]. Here we show that SWELL1 (LRRC8a) mediates a swell-activated, depolarizing chloride current ($I_{Cl,SWELL}$) in β-cells. Hypotonic and glucose-stimulated β-cell swelling activates SWELL1-mediated $I_{Cl,SWELL}$ and this is required for both glucose-stimulated and hypotonic swell-mediated activation of VGCC-dependent intracellular calcium signaling in β-cells. SWELL1 KO MIN6 cells and β-cell targeted SWELL1 KO murine islets exhibit significantly impaired glucose-stimulated insulin secretion, with preserved insulin content *in vitro*. Tamoxifen-inducible β-cell targeted *SWELL1* KO mice have normal fasting insulin levels but display markedly impaired glucose-stimulated insulin secretion. Our results reveal a physiological role for SWELL1 as a glucose sensor - linking glucose-mediated β-cell swelling to SWELL1-dependent activation of VGCC-triggered calcium signaling, and highlights SWELL1-mediated "swell-secretion" coupling as required for glucose-stimulated insulin secretion.

## MAIN

Recent studies have identified SWELL1 (LRRC8a) as a required component of a swell-activated $Cl^-$ current $I_{Cl,SWELL}$ or ***V***olume-***R***egulated ***A***nion ***C***urrent (VRAC) in common cell lines[11, 12], forming multimeric channels with LRRC8b-e[13]. To determine if SWELL1 is also required for VRAC in pancreatic β-cells we suppressed SWELL1 in mouse insulinoma (MIN6) cells by adenoviral transduction with an shRNA-directed against SWELL1 (Ad-U6-shSWELL1-mCherry; Fig. 1a) as compared to a scrambled shRNA control (Ad-U6-shSCR-mCherry). We observed robust knock-down of SWELL1 protein (Fig. 1b) and a significant reduction in hypotonic swell-activated VRAC in Ad-shSWELL1 relative to Ad-shSCR transduced MIN6 cells (Fig. 1c&d). To determine whether SWELL1 is also required for VRAC in mouse primary β-cells we isolated islets from *SWELL1* floxed mice (*SWELL1*$^{fl}$)[14] and transduced them with an adenovirus expressing GFP under control of a rat insulin promoter (Ad-RIP2-GFP) to allow positive identification of β-cells (GFP+ cells). *SWELL1*$^{fl}$ islets were further treated with adenovirus expressing Cre-mCherry to allow Cre-mediated excision of the floxed SWELL1 allele or control virus expressing mCherry alone (Supplementary Fig. 1a). By selecting GFP+/mCherry+ cells, we are able to patch-clamp either control WT β-cells (*SWELL1*$^{fl}$ β-cells) or *SWELL1* KO β-cells (*SWELL1*$^{fl}$/Cre β-cells; Fig. 1e). We find that WT β-cells express substantial swell-activated current and this is entirely abolished upon Cre-mediated recombination in *SWELL1* KO β-cells (Fig. 1f-h). We next tested whether SWELL1 is also required for VRAC in human β-cells and applied a similar approach. We transduced human islets with Ad-RIP2-GFP and Ad-shSWELL1-mCherry or Ad-sh-SCR-mCherry (Supplementary Fig. 1b), in order to isolate and patch-clamp human β-cells (GFP+) subjected to shRNA-mediated SWELL1 KD or to a scrambled control (GFP+/mCherry+; Fig. 1i). Similar to mouse β-cell recordings we find that human β-cells also express significant SWELL1-mediated swell-activated current (Fig. 1j-l). Indeed, in all β-cells patch-clamped, the reversal potential was ~-12 mV, which is near the reversal potential for $Cl^-$ under our recording conditions, and thus consistent with SWELL1-mediating a swell-activated $Cl^-$ conductance in β-cells[15-17]. These data demonstrate that SWELL1 is required for VRAC or $I_{Cl,SWELL}$ in pancreatic β-cells.

Having established that SWELL1 is required for this previously enigmatic depolarizing swell-activated $Cl^-$ current[16, 17] in MIN6 cells, and in both mouse and human primary β-cells we asked whether physiologic glucose-mediated β-cell swelling[18] is sufficient to activate SWELL1-mediated VRAC. First, we measured β-cell size by light microscopy in WT and SWELL1-deficient primary murine and human β-cells in response to glucose-stimulated swelling (at 35-37°C). WT murine β-cells swell 6.8 ± 1.6 % in cross-sectional area upon perfusion of 16.7 mM glucose (from 1 mM basal glucose) and reach a maximum size at 12 minutes post glucose-stimulation, followed by a reduction in β-cell size (Fig. 2a), consistent with regulatory volume decrease (RVD). In contrast, SWELL1 KO murine β-cells swell monotonically to 8.2 ± 2.4 % and exhibit no RVD (Fig. 2a). WT human β-cells show a similar trend, swelling 8.6 ± 3.5 %, followed by RVD (Fig. 2b). SWELL1 KD human β-cells swell monotonically to 6.0 ± 1.5 % (Fig. 2b), and similar to SWELL1 KO murine β-cells (Fig. 2a), exhibit no RVD. These data indicate that physiological increases in glucose induce β-cell swelling and that SWELL1 is required for RVD in primary β-cells, as observed in cell lines[11, 12, 19]. Next, we applied the perforated-patch clamp technique to primary β-cells at 35-37°C in order to measure currents under the same physiological conditions that induce glucose-mediated β-cell swelling. We find that β-cell VRAC activates in response to physiological increases in glucose in MIN6 cells (Supplementary Fig. 2) and in both mouse (Fig. 2c-d) and human (Fig. 2e-f) β-cells, and is blocked by the selective VRAC inhibitor, DCPIB. Importantly, the time-course of VRAC activation in β-cells either tracks or lags the latency of β-cell swelling in response to stimulatory glucose (~8 minutes), consistent with a mechanism of glucose-mediated β-cell swell-activation of SWELL1-mediated VRAC. Thus, SWELL1-mediates a glucose-sensitive swell-activated depolarizing $Cl^-$ current in β-cells.

To determine whether SWELL1-mediated depolarizing $Cl^-$ current is required to depolarize the β-cell membrane potential to the activation threshold of voltage-gated $Ca^{2+}$ channels (VGCC) essential for insulin granule fusion, we next measured glucose-stimulated intracellular $Ca^{2+}$ in WT and SWELL1 -deficient MIN6 β-cells, primary mouse and human β-cells. Using CRISPR/cas9 technology, we generated multiple SWELL1 KO MIN6 cell lines (Supplementary Fig. 3), confirming *SWELL1* gene

disruption by PCR (Supplementary Fig. 3a), SWELL1 protein deletion (Fig. 3a & Supplementary Fig. 3b) and ablation of SWELL1-mediated current (Fig. 3b) in these cells. We find that glucose-stimulated $Ca^{2+}$ transients are entirely abolished in SWELL1 KO MIN6 compared to WT cells (Fig. 3c-e), despite preserved KCl (40 mM) stimulated $Ca^{2+}$ transients (control for intact β-cell excitability). Co-application of a selective VGCC blocker nifedipine (10 μM) fully inhibits these glucose-stimulated $Ca^{2+}$ transients in WT MIN6 cells, consistent with a mechanism of membrane depolarization and VGCC activation (Supplementary Fig. 4a&b).

As β-cells are also known to depolarize, fire $Ca^{2+}$ transients, and secrete insulin via a glucose-independent hypotonic swelling mechanism[16, 20], we next examined swell-induced $Ca^{2+}$-signaling in β-cells in response to hypotonic stimulation (220 mOsm) in the absence of glucose-stimulation (0 mM glucose). We find that hypotonic swelling alone can trigger robust $Ca^{2+}$ transients in WT MIN6 cells (Fig. 3f&h) and these elevations in cytosolic $Ca^{2+}$ recover rapidly upon restoration of isotonic solution (Fig. 3f). In contrast, SWELL1 KO MIN6 cells are entirely non-responsive to hypotonic swelling induced $Ca^{2+}$ transients (Fig. 3f-h), despite preserved KCl stimulated $Ca^{2+}$ responses, consistent with SWELL1-mediating a glucose-independent, swell-activated depolarizing current in β-cells. Similar to the case with glucose-stimulated $Ca^{2+}$ signaling, we also find that hypotonic swelling triggered $Ca^{2+}$ transients are fully inhibited by VGCC blockade (Supplementary Fig. 4c&d), implicating β-cell membrane depolarization followed by VGCC activation, as opposed to alternative hypo-osmotically activated $Ca^{2+}$ influx pathways (i.e. TRP channels)[21].

We next examined SWELL1-dependent $Ca^{2+}$ signaling in primary mouse and human β-cells. We generated adenoviruses expressing the genetically encoded $Ca^{2+}$-sensor GCaMP6s under control of the rat insulin promoter 1 (RIP1), either alone (Ad-RIP1-GCaMP6s), or in combination with Cre-recombinase (Ad-RIP1-Cre-P2A-GCaMP6s). This approach provides a robust β-cell restricted fluorescent $Ca^{2+}$ sensor while simultaneously allowing for β-cell targeted Cre-mediated *SWELL1* deletion in cultured *SWELL1*$^{fl/fl}$ islets isolated from *SWELL1*$^{fl/fl}$ mice (Fig. 3i). GCaMP6s $Ca^{2+}$ imaging reveals robust glucose-stimulated $Ca^{2+}$ transients in freshly dissociated WT primary murine β-cells *(*Ad-

RIP1-GCaMP6s/*SWELL1*$^{fl/fl}$; Fig. 3j&l) and these are significantly suppressed in SWELL1 KO β-cells (Ad-RIP1-Cre-P2A-GCaMP6s/*SWELL1*$^{fl/fl}$; Fig. 3k&l), despite preserved KCl stimulated $Ca^{2+}$ responses. We used a similar approach in human islets, whereby we co-transduced islets with Ad-RIP1-GCaMP6s (Fig. 3m) and either Ad-U6-shSWELL1-mCherry or Ad-U6-shSCR-mCherry. Upon islet dissociation, we imaged only double-labelled GCaMP6s+/mCherry+ primary human β-cells. As with mouse primary β-cells, we observe robust glucose-stimulated $Ca^{2+}$ transients in Ad-shSCR treated human primary β-cells (Fig. 3n&p) and this is markedly abograted upon Ad-shSWELL1-mediated SWELL1 knock-down (Fig. 3o&p). Collectively, these data demonstrate that SWELL1 is required for both glucose- and swell-activated $Ca^{2+}$ signaling in MIN6 cells and in mouse and human primary β-cells. Moreover, these data suggest that the depolarizing SWELL1-mediated $Cl^-$ current is necessary for β-cell depolarization in response to glucose-stimulation. In pancreatic β-cells, physiological intracellular $Cl^-$ concentration is maintained at 34-36 mM[22, 23] by NKCC1 transporters[24, 25] to generate a depolarizing $Cl^-$ current upon activation of a $Cl^-$ conductance, since $E_{Cl-}$ = ~-35 mV. Therefore, NKCC1 blockade by bumetanide[26, 27] is predicted to reduce intracellular $Cl^-$, drop $E_{Cl-}$ and thereby diminish or abolish β-cell membrane depolarization by a SWELL1-mediated glucose-stimulated $Cl^-$ conductance. Consistent with this prediction, we find that application of bumetanide (10 μM) fully inhibits glucose-stimulated $Ca^{2+}$ signaling in both WT MIN6 cells (Supplementary Fig. 4e&f) and WT primary murine β-cells (Supplementary Fig. 4g&h).

To determine the impact of SWELL1-dependent glucose-stimulated $Ca^{2+}$ signaling on insulin secretion in β-cells we measured glucose-stimulated insulin secretion (GSIS) in WT and SWELL1 KO MIN6 cells. We find that the glucose-dependent increase in insulin secretion in WT MIN6 cells is significantly diminished in SWELL1 KO MIN6 cells (Fig. 4a), particularly at higher glucose concentration (30 mM), despite no change in total insulin content (Fig. 4b). We next isolated islets from *SWELL1*$^{fl/fl}$ mice followed by transduction with either Ad-RIP1-RFP (WT) or Ad-RIP1-Cre-P2A-RFP (SWELL1 KO; Fig. 4c). Similar to MIN6 cells, we note a significant reduction in GSIS (16.7 mM glucose) in SWELL1

KO compared to WT islets (Fig. 4d), despite relatively preserved L-arginine stimulated insulin secretion (Fig. 4d), and similar total insulin content (Fig. 4e).

We next generated tamoxifen-inducible β-cell-targeted *SWELL1* KO mice by crossing *SWELL1*$^{fl/fl}$ mice with *Ins1Cre*$^{ERT2}$ mice (*KO Ins1Cre*$^{ERT2}$, Fig. 4f) [28] to examine the requirement of β-cell SWELL1 for insulin secretion *in vivo*. After tamoxifen-administration (40-80 mg/kg/day x 5 days), we observe pancreas-restricted *SWELL1* recombination in *KO Ins1Cre*$^{ERT2}$ mice by PCR across *SWELL1* Exon 3 (426 bp amplicon; Fig. 4g) and complete ablation of SWELL1-mediated current in 80% of patch-clamped β-cells (8/10 cells; Fig. 4h-i), while 100% of β-cells from tamoxifen-induced *SWELL1*$^{fl/fl}$ (WT) had robust hypotonically-activated SWELL1-mediated currents (4/4 cells). We find that basal (fasting) serum insulin are similar between WT and *KO Ins1Cre*$^{ERT2}$ mice (Fig. 4j), which is consistent with preserved basal insulin secretion observed at low glucose *in vitro* in SWELL1 KO MIN6 cells (Fig. 4a) and in β-cell-targeted SWELL1 KO murine islets (Fig. 4d). However, with glucose-stimulation (2 g/kg i.p.) we find that insulin secretion is significantly impaired in *KO Ins1Cre*$^{ERT2}$ mice compared to WT mice (Fig. 4j). Overall, these data are consistent with a requirement of β-cell SWELL1 for glucose-stimulated, $Ca^{2+}$-dependent insulin secretion both *in vitro* and *in vivo*.

VRAC/$I_{Cl,SWELL}$ has been studied for decades through electrophysiological recordings in numerous cell types[29-31], but only recently has it been discovered that SWELL1/LRRC8a, and associated LRRC8 isoforms b-e, form the VRAC channel complex in common cell lines[11-13]. Accordingly, the physiological role of SWELL1-mediated VRAC in primary cells remains unexplored. We recently showed that SWELL1 is required for VRAC in adipocytes where it senses adipocyte hypertrophy in the setting of obesity and regulates insulin-PI3K-AKT2-GLUT4 mediated glucose uptake and systemic glycemia [32]. Here we asked whether SWELL1 is required for VRAC described previously in the pancreatic β-cell [16-18] and whether the VRAC hypothesis [33] can be explained by a putative glucose-mediated swell sensing function of the SWELL1/LRRC8 channel complex in β-cells. Indeed, our data are consistent with a model in which SWELL1 is a required component of a swell-activated depolarizing $Cl^-$ channel that

activates in response to glucose-stimulated β-cell swelling and is required for membrane depolarization, VGCC activation, $Ca^{2+}$-mediated insulin vesicle fusion and insulin secretion. In this model, the hyperpolarizing $K^+$ conductances [4-10] act as a "brakes" on β-cell excitability and insulin secretion, while SWELL1-mediated VRAC is the "accelerator" - promoting β-cell excitability in response to glucose-mediated β-cell swelling. Overall, these data suggest that β-cell SWELL1 acts as a glucose sensor by coupling β-cell swelling to β-cell depolarization - a form of swell-activation or swell-secretion coupling - to potentiate glucose-stimulated insulin secretion. In the broader context of our findings on SWELL1 signaling in the adipocyte [32], these data suggest that SWELL1 coordinately regulates both insulin secretion and insulin sensitivity [32] in response to a nutrient load, highlighting the importance SWELL1 in the regulation of systemic glucose metabolism.

## AUTHOR CONTRIBUTIONS

Conceptualization, R.S.; Methodology, C.K., S.B.S., A.W.N., A.M., Y.Z., L.X., S.K.G., S.P. Y.G. R.S.; Formal Analysis, C.K., R.S.; Investigation, C.K., S.S., A.M., S.P., Y.G.; Resources, R.S., A.W.N.; Writing – Original Draft, R.S., Writing – Review & Editing, R.S., C.K., S.B.S, A.W.N.; Visualization, C.K., R.S.; Supervision, R.S.; Funding Acquisition, R.S.

## ACKNOWLEDGMENTS

We thank Dr. John Engelhardt for sharing human islets obtained from the Integrated Islet Distribution Program (IIDP) and Dr. Yumi Imai sharing human islets obtained from Prodo Laboratories. We thank Shanming Hu for assisting with mouse islet isolations and Dr. Robert Tsushima for thoughtful reading of the manuscript and comments. This work was supported by grants from the NIH NIDDK 1R01DK106009 (R.S.), R01DK097820 (A.W.N.), R24DK96518 (A.W.N.) and the Roy J. Carver Trust (R.S.).

**Figure 1. *SWELL1* mediates VRAC in MIN6 cells and primary mouse and human pancreatic β-cells**

**a**, mCherry fluorescence of the mouse insulinoma cell line (MIN6) transduced with an adenovirus expressing a short-hairpin RNA directed to SWELL1 (shSWELL1-mCherry). **b**, SWELL1 Western blot in MIN6 cells transduced with shSWELL1 compared to scrambled short-hairpin RNA (shSCR). β-actin loading control (Supplementary Fig. 5 for full blots). **c**, Current-voltage relationship of VRAC in MIN6 cells at baseline (black) and after hypotonic swelling (Hypo, 210 mOsm, blue) after adenoviral transduction with shSCR (left) and shSWELL1 (right). **d**, Mean current inward and outward densities at +100 and -100 mV ($n_{shSCR}$ = 3 cells; $n_{shSWELL1}$ = 4 cells). **e**, Bright-field, GFP, mCherry and merged images of freshly dispersed primary β-cells from *SWELL1*$^{fl/fl}$ mouse islets co-transduced with Ad-RIP1-GFP and Ad-Cre-mCherry. (**f-g)**, Current-time relationship (**f**) and current-voltage relationship (**g**) of swell-activated VRAC in wild-type (WT: Ad-mCherry/*SWELL1*$^{fl/fl}$) and SWELL1 knockout (KO: Ad-Cre-mCherry/*SWELL1*$^{fl/fl}$) mouse primary β-cells. (**h**) Mean current inward and outward densities at +100 and -100 mV (n = 5 cells, each group). (**i**) Bright-field, GFP, mCherry and merged images of freshly dispersed primary β-cells from human islets co-transduced with Ad-RIP1-GFP and Ad-shSWELL1-mCherry. (**j**) Current-time relationship and (**k**) current-voltage relationship of swell-activated VRAC in WT and SWELL1 knockdown primary human β-cells. (**l**) Mean current inward and outward densities at +100 and -100 mV ($n_{shSCR}$ = 5 cells; $n_{shSWELL1}$ = 10 cells). Ramp protocol is from +100 mV to -100 mV (ramp duration: 600 ms, holding potential: 0 mV). Error bars in d, h, and l denote ± s.e.m. * P < 0.05; **P < 0.01; *** P < 0.001, unpaired t-test.

**Figure 2. β-cell VRAC is activated by physiological swelling in response to glucose stimulation.**

**a-b**, Cross-sectional area of primary WT (n = 12) and SWELL1 KO (n = 7) murine β-cells (**a**) and WT (n = 9) and SWELL1 KD (n = 8) human β-cells (**b**) in response to glucose-stimulation (1, 16.7, 1 mM glucose). **c-d**, Murine primary β-cell VRAC over time (**c**) and current-voltage relationship (**d**) with

DCPIB inhibition (10 uM). **e-f**, Human primary β-cell VRAC over time (**e**) and current-voltage relationship (**f**) with DCPIB inhibition (10 uM). Recordings in **c-f** performed at 35-37$^{o}$C in perforated-patch configuration. In (a), **P < 0.01 vs 0 min in WT, paired t-test; $^{\$}$P < 0.05 vs 0 min in SWELL1 KO, paired-test; $^{\#}$P < 0.05 WT vs SWELL1 KO, unpaired t-test. In (b), *P < 0.05 vs 0 min in WT, paired t-test; $^{\$}$P < 0.05 vs 0 min in SWELL1 KD, paired-test; $^{\#\#}$P < 0.01 WT vs SWELL1 KD, unpaired t-test.

**Figure 3. *SWELL1*-mediated VRAC is required for both glucose- and hypotonic swelling induced $Ca^{2+}$ signaling in β-cells.**

**a**, SWELL1 Western blot in WT and CRISPR/Cas9-mediated SWELL1 KO MIN6 cell lines (Supplementary Fig. 5 for full blots). **b**, Current-voltage plots of SWELL1-mediated current in response to hypotonic swelling in WT and SWELL1 KO MIN6 cells confirm complete ablation of hypotonic swelling stimulated VRAC in SWELL1 KO MIN6 cells. (**c-d**) Fura-2 $Ca^{2+}$ transients in WT (**c**) and SWELL1 KO (**d**) MIN6 cells in response to 30 mM glucose-stimulation (basal 1 mM glucose). 40 mM KCl stimulation confirms cell viability and excitability. (**e**) Mean peak Fura-2 ratio in glucose-stimulated WT (n = 34) and SWELL1 KO (n= 36) MIN6 cells. (**f-g**) Fura-2 $Ca^{2+}$ transients in WT (**f**) and SWELL1 KO (**g**) MIN6 cells in response to swell-stimulation (210 mOsm; isotonic 300 mOsm). (**h**) Mean peak Fura-2 ratio in swell-stimulated WT (n = 42) and SWELL1 KO (n = 26) MIN6 cells. (**i**) Ad-RIP1-GCaMP6s transduced SWELL1$^{fl/fl}$ murine islet. (**j-k**) GCaMP6s $Ca^{2+}$ transients in WT (J, Ad-RIP1-GCaMP6s/SWELL1$^{fl/fl}$) and SWELL1 KO (K, Ad-RIP1-Cre-P2A-GCaMP6s/SWELL1$^{fl/fl}$) primary murine β-cell in response to 16.7 mM glucose-stimulation (basal 1 mM glucose). 40 mM KCl stimulation. Insets show β-cell fluorescence images at the indicated times in the experiment. (**l**) Mean peak values of GCaMP6s $Ca^{2+}$ transients from Ad-RIP1-GCaMP6s/SWELL1$^{fl/fl}$ (n = 14) and Ad-RIP1-Cre-P2A-GCaMP6s/SWELL1$^{fl/fl}$ (n = 10). (**m**) Ad-RIP1-GCaMP6s transduced human islet. (**o-p**) GCaMP6s $Ca^{2+}$ transients in human primary β-cell co-transduced with Ad-RIP1-GCaMP6s+Ad-shSCR-mCherry (**o**) and Ad-RIP1-GCaMP6s+Ad-shSWELL1-mCherry (**p**) in response to 16.7 mM glucose-stimulation (basal 1 mM glucose). 40 mM KCl stimulation. (**q**) Mean peak values of GCaMP6s $Ca^{2+}$ transients from shSCR (n = 6) and shSWELL1 (n = 8). Error bars represent mean ± SEM, **p < 0.01, ***p < 0.001.

**Figure 4. . β-cell *SWELL1* is required for glucose-stimulated insulin secretion *in vitro* and *in vivo***

**a**, Glucose-stimulated insulin secretion (GSIS) in WT and SWELL1 KO MIN6 cells in response to 1, 5.5 and 30 mM glucose (n = 3, each). **b**, Total insulin content normalized to total MIN6 cell protein content (n = 3, each). **c**, Representative image of Ad-RIP1-Cre-RFP transduced mouse islet. **d**, GSIS in WT (Ad-RIP1-RFP/*SWELL1*$^{fl/fl}$) and β-cell targeted SWELL1 KO (Ad-RIP1-Cre-RFP/*SWELL1*$^{fl/fl}$) islets. Insulin secretion is expressed as percentage of the total insulin content (n = 4, each). **e**,Total insulin content of WT and β-cell targeted SWELL1 KO islets (n = 4, each). (**f**) Tamoxifen-inducible β-cell-targeted *SWELL1* inactivation using *Ins1Cre*$^{ERT2}$ mouse crossed with *SWELL1*$^{fl/fl}$ mice (*KO Ins1Cre*$^{ERT2}$). (**g**) PCR across *SWELL1* Exon 3 in genomic DNA extracted from pancreas, liver and adipose tissues of a *KO Ins1Cre*$^{ERT2}$ mouse treated with (+) and without (-) tamoxifen. *Cre*-mediated *SWELL1* recombination results in a 426 bp amplicon. (**h**) Current-voltage relationship of swell-activated VRAC in mouse primary β-cells isolated from *SWELL1*$^{fl/fl}$ +tamoxifen (WT) and *KO Ins1Cre*$^{ERT2}$ +tamoxifen (*KO Ins1Cre*$^{ERT2}$). (**i**) Mean inward and outward current densities at +100 and -100 mV (n = 4 cells for WT and n = 10 cells for *KO Ins1Cre*$^{ERT2}$). (**j**) Glucose-stimulated insulin secretion in WT and *KO Ins1Cre*$^{ERT2}$ mice in response to 2g/kg glucose in the first 30 min (n = 8, male, for each group). Error bars represent mean ± SEM, * $p < 0.05$; ** $p < 0.01$; *** $p < 0.001$ vs. WT; ns: not statistically significant, one-way ANOVA for in-group comparison, unpaired t-test for between-group comparison. For (**j**), non-parametric one-way ANOVA (Kruskal Wallis test) was performed. Error bars represent mean ± SEM, * $p < 0.05$; ** $p < 0.01$; *** $p < 0.001$ vs. WT (30 mM glucose); ns: not statistically significant

**Supplementary Figure 1: Fluorescence images of adenovirally transduced murine and human islets**

**a**, Murine islets freshly isolated from SWELL1$^{fl/fl}$ mice, cultured (BF: Bright field) and then co-transduced with Ad-RIP1-GFP (GFP) and Ad-CMV-mCherry (top, cytosolic mCherry: Control) or Ad-CMV-Cre-mCherry (bottom: nuclear-localized Cre-mCherry fusion protein; SWELL1 KO).

283 **b**, Human islets cultured (BF: Bright field) and then co-transduced with Ad-RIP1-GFP (GFP) and Ad-
284 U6-shSCR-mCherry (top, mCherry: Control) or Ad-U6-shSWELL1-mCherry (bottom: mCherry; SWELL1
285 KD). Scale bar represents 50 μm.
286
287
288 **Supplementary Figure 2: MIN6 β-cell VRAC is activated by glucose stimulation**
289 Glucose-stimulated VRAC recorded in patch-clamped MIN6 β-cell upon application of 30 mM glucose
290 from a basal glucose of 1 mM. Recordings performed at 35-37$^{o}$C in perforated-patch configuration.
291
292 **Supplementary Figure 3: CRISPR/cas9-mediated *SWELL1* ablation in MIN6 cells**
293 **a**, Guide RNA sequences targeting exon 3 of the *SWELL1* gene were used in combinations of either
294 1A+2B or 2B+3C to generate KO1 and KO2 clones respectively. Upon interacting with *cas9* enzyme
295 and corresponding guide pairs the target region undergoes non-homologous end joining (NHEJ) repair.
296 This results in the deletion of DNA base pairs in-between the two target guide sites. Using specific
297 primers for the regions flanking the two target guide sites, the wildtype, WT (non-transfected) cells
298 generate a fragment of size 661 and 879 bps for the 1A/2B and 2B/3C sites respectively, upon PCR
299 amplification. The KO1 and KO2 clones (transfected) generate a deleted DNA fragment of size
300 approximately 410 and 639 bps for the 1A/2B and 2B/3C sites respectively. In the agarose gel image,
301 the DNA fragment sizes are indicated in base-pairs (bp) and 'L' indicates ladder. **b,** Western-blot of
302 SWELL1 protein in WT (non-transfected, WT1, WT2) and multiple SWELL1 KO MIN6 clones (KO1-5).
303 ß-actin is used as the loading control (Supplementary Fig. 5 for full blots).
304
305 **Supplementary Figure 4: Glucose and hypotonic swell-stimulated $Ca^{2+}$ signaling is dependent**
306 **on VGCC and elevated intracellular chloride in β-cells**
307 **a**, Fura-2 $Ca^{2+}$ transients in WT MIN6 cells in response to 30 mM glucose-stimulation (basal 1 mM
308 glucose) in the presence of VGCC blocker nifedipine (10 μM). **b**, Mean peak Fura-2 ratio from **a** (n = 16
309 cells). **c**, Fura-2 $Ca^{2+}$ transients in WT MIN6 cells in response to hypotonic swelling (210 mOsm;

isotonic 300 mOsm) in the presence of VGCC blocker nifedipine (10 μM). **d**, Mean peak Fura-2 ratio from **c** (n = 43 cells). **e**, Fura-2 $Ca^{2+}$ transients in WT MIN6 cells in response to 30 mM glucose-stimulation (basal 1 mM glucose) in the presence of NKCC1 inhibitor, bumetanide (10 μM). **f**, Mean peak Fura-2 ratio from **e** (n = 46 cells). **g**, GCaMP6s $Ca^{2+}$ transients in WT (Ad-RIP1-GCaMP6s/SWELL1$^{fl/fl}$) primary murine β-cell in response to 16.7 mM glucose-stimulation (basal 1 mM glucose) in the presence of NKCC1 inhibitor, bumetanide (10 μM). **h**, Mean peak values of GCaMP6s $Ca^{2+}$ transients from **g** (n = 7 cells). In all experiments, 40 mM KCl stimulation confirms cell viability and excitability. Error bars represent mean ± s.e.m., **p < 0.01; ***p < 0.001; ns: not statistically significant.

## References


1. Yang, S.N. *et al.* Ionic mechanisms in pancreatic beta cell signaling. *Cell Mol Life Sci* **71**, 4149-4177 (2014).
2. Rorsman, P. & Braun, M. Regulation of insulin secretion in human pancreatic islets. *Annu Rev Physiol* **75**, 155-179 (2013).
3. Rorsman, P., Eliasson, L., Kanno, T., Zhang, Q. & Gopel, S. Electrophysiology of pancreatic beta-cells in intact mouse islets of Langerhans. *Prog Biophys Mol Biol* **107**, 224-235 (2011).
4. Nichols, C.G. KATP channels as molecular sensors of cellular metabolism. *Nature* **440**, 470-476 (2006).
5. Ashcroft, F.M. & Rorsman, P. K(ATP) channels and islet hormone secretion: new insights and controversies. *Nat Rev Endocrinol* **9**, 660-669 (2013).
6. MacDonald, P.E. *et al.* Members of the Kv1 and Kv2 voltage-dependent K(+) channel families regulate insulin secretion. *Molecular endocrinology* **15**, 1423-1435 (2001).
7. Jacobson, D.A. *et al.* Kv2.1 ablation alters glucose-induced islet electrical activity, enhancing insulin secretion. *Cell metabolism* **6**, 229-235 (2007).
8. Tamarina, N.A., Kuznetsov, A., Fridlyand, L.E. & Philipson, L.H. Delayed-rectifier (KV2.1) regulation of pancreatic beta-cell calcium responses to glucose: inhibitor specificity and modeling. *American journal of physiology. Endocrinology and metabolism* **289**, E578-585 (2005).
9. Dadi, P.K., Vierra, N.C. & Jacobson, D.A. Pancreatic beta-cell-specific ablation of TASK-1 channels augments glucose-stimulated calcium entry and insulin secretion, improving glucose tolerance. *Endocrinology* **155**, 3757-3768 (2014).
10. Vierra, N.C. *et al.* Type 2 Diabetes-Associated K+ Channel TALK-1 Modulates beta-Cell Electrical Excitability, Second-Phase Insulin Secretion, and Glucose Homeostasis. *Diabetes* **64**, 3818-3828 (2015).
11. Qiu, Z. *et al.* SWELL1, a Plasma Membrane Protein, Is an Essential Component of Volume-Regulated Anion Channel. *Cell* **157**, 447-458 (2014).
12. Voss, F.K. *et al.* Identification of LRRC8 heteromers as an essential component of the volume-regulated anion channel VRAC. *Science* **344**, 634-638 (2014).
13. Syeda, R. *et al.* LRRC8 Proteins Form Volume-Regulated Anion Channels that Sense Ionic Strength. *Cell* **164**, 499-511 (2016).
14. Zhang, Y. *et al.* SWELL1 is a regulator of adipocyte size, insulin signaling and glucose homeostasis. *Nature cell biology* **Accepted, in press** (2017).

15. Best, L. Glucose-induced electrical activity in rat pancreatic beta-cells: dependence on intracellular chloride concentration. *J Physiol* **568**, 137-144 (2005).
16. Best, L., Miley, H.E. & Yates, A.P. Activation of an anion conductance and beta-cell depolarization during hypotonically induced insulin release. *Exp Physiol* **81**, 927-933 (1996).
17. Best, L., Sheader, E.A. & Brown, P.D. A volume-activated anion conductance in insulin-secreting cells. *Pflugers Arch* **431**, 363-370 (1996).
18. Miley, H.E., Sheader, E.A., Brown, P.D. & Best, L. Glucose-induced swelling in rat pancreatic beta-cells. *J Physiol* **504 ( Pt 1)**, 191-198 (1997).
19. Planells-Cases, R. *et al.* Subunit composition of VRAC channels determines substrate specificity and cellular resistance to Pt-based anti-cancer drugs. *EMBO J* **34**, 2993-3008 (2015).
20. Sheader, E.A., Brown, P.D. & Best, L. Swelling-induced changes in cytosolic [Ca2++] in insulin-secreting cells: a role in regulatory volume decrease? *Mol Cell Endocrinol* **181**, 179-187 (2001).
21. Liedtke, W., Tobin, D.M., Bargmann, C.I. & Friedman, J.M. Mammalian TRPV4 (VR-OAC) directs behavioral responses to osmotic and mechanical stimuli in Caenorhabditis elegans. *Proc Natl Acad Sci U S A* **100 Suppl 2**, 14531-14536 (2003).
22. Eberhardson, M., Patterson, S. & Grapengiesser, E. Microfluorometric analysis of Cl- permeability and its relation to oscillatory Ca2+ signalling in glucose-stimulated pancreatic beta-cells. *Cell Signal* **12**, 781-786 (2000).
23. Sehlin, J. Interrelationship between chloride fluxes in pancreatic islets and insulin release. *Am J Physiol* **235**, E501-508 (1978).
24. Lindstrom, P., Norlund, L., Sandstom, P.E. & Sehlin, J. Evidence for co-transport of sodium, potassium and chloride in mouse pancreatic islets. *J Physiol* **400**, 223-236 (1988).
25. Sandstrom, P.E. & Sehlin, J. Evidence for separate Na+, K+, Cl- and K+, Cl- co-transport systems in mouse pancreatic beta-cells. *Eur J Pharmacol* **238**, 403-405 (1993).
26. Sandstrom, P.E. Evidence for diabetogenic action of bumetanide in mice. *Eur J Pharmacol* **150**, 35-41 (1988).
27. Sandstrom, P.E. Bumetanide reduces insulin release by a direct effect on the pancreatic beta-cells. *Eur J Pharmacol* **187**, 377-383 (1990).
28. Magnuson, M.A. & Osipovich, A.B. Pancreas-specific Cre driver lines and considerations for their prudent use. *Cell metabolism* **18**, 9-20 (2013).
29. Strange, K., Emma, F. & Jackson, P.S. Cellular and molecular physiology of volume-sensitive anion channels. *Am J Physiol* **270**, C711-730 (1996).
30. Okada, Y. Volume expansion-sensing outward-rectifier Cl- channel: fresh start to the molecular identity and volume sensor. *Am J Physiol* **273**, C755-789 (1997).
31. Okada, Y., Sato, K. & Numata, T. Pathophysiology and puzzles of the volume-sensitive outwardly rectifying anion channel. *J Physiol* **587**, 2141-2149 (2009).
32. Zhang, Y. *et al.* SWELL1 is a regulator of adipocyte size, insulin signalling and glucose homeostasis. *Nature cell biology* (2017).
33. Best, L., Brown, P.D., Sener, A. & Malaisse, W.J. Electrical activity in pancreatic islet cells: The VRAC hypothesis. *Islets* **2**, 59-64 (2010).

**Figure 1**

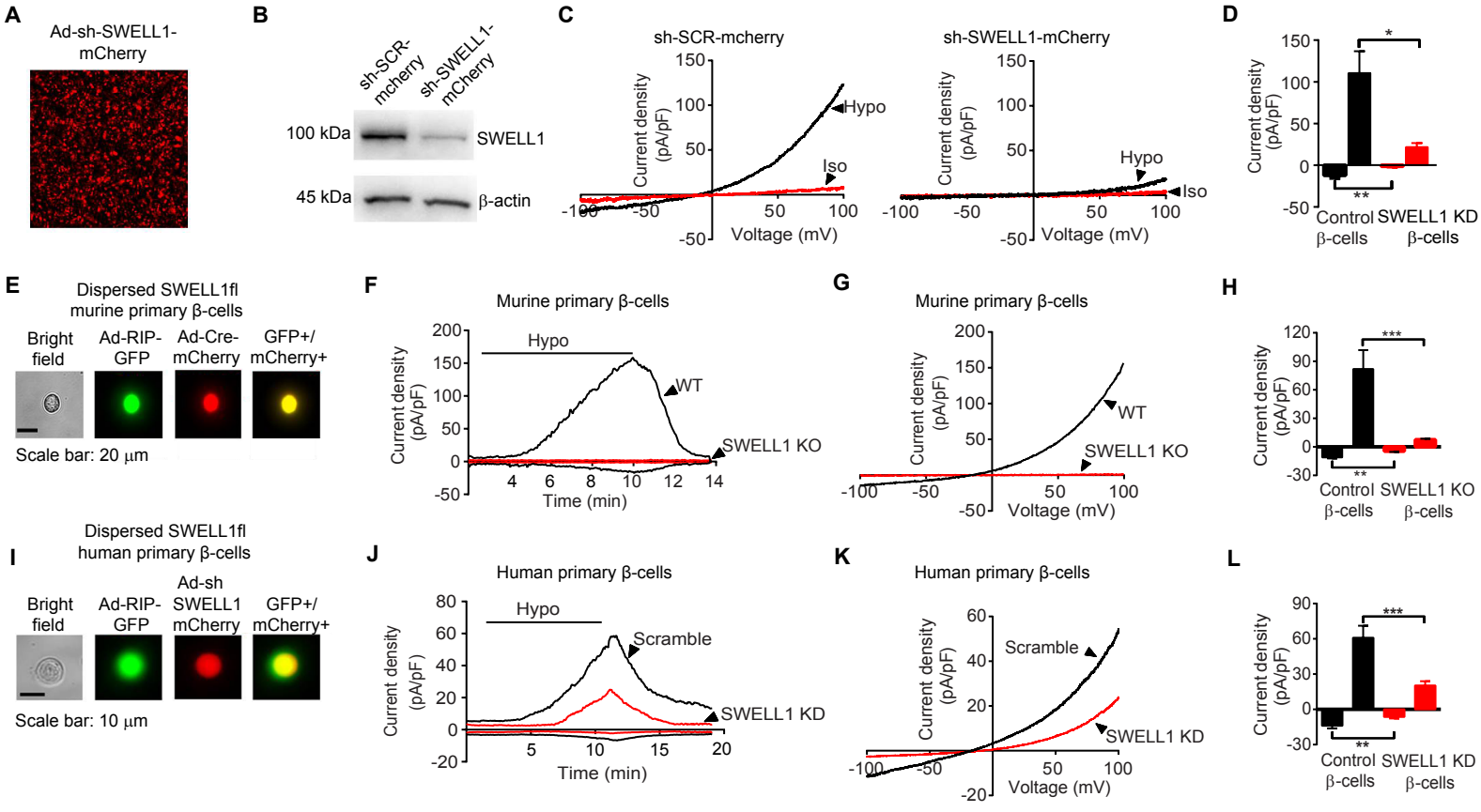
A
Ad-sh-SWELL1-mCherry
B
sh-SCR-mcherry
sh-SWELL1-mCherry
100 kDa
SWELL1
45 kDa
β-actin
C
sh-SCR-mcherry
sh-SWELL1-mCherry
Current density (pA/pF)
Hypo
Iso
Voltage (mV)
D
Current density (pA/pF)
Control β-cells
SWELL1 KD β-cells
E
Dispersed SWELL1fl murine primary β-cells
Bright field
Ad-RIP-GFP
Ad-Cre-mCherry
GFP+/ mCherry+
Scale bar: 20 μm
F
Murine primary β-cells
Hypo
WT
SWELL1 KO
Current density (pA/pF)
Time (min)
G
Murine primary β-cells
WT
SWELL1 KO
Current density (pA/pF)
Voltage (mV)
H
Current density (pA/pF)
Control β-cells
SWELL1 KO β-cells
I
Dispersed SWELL1fl human primary β-cells
Bright field
Ad-RIP-GFP
Ad-sh SWELL1 mCherry
GFP+/ mCherry+
Scale bar: 10 μm
J
Human primary β-cells
Hypo
Scramble
SWELL1 KD
Current density (pA/pF)
Time (min)
K
Human primary β-cells
Scramble
SWELL1 KD
Current density (pA/pF)
Voltage (mV)
L
Current density (pA/pF)
Control β-cells
SWELL1 KD β-cells

**Figure 2**

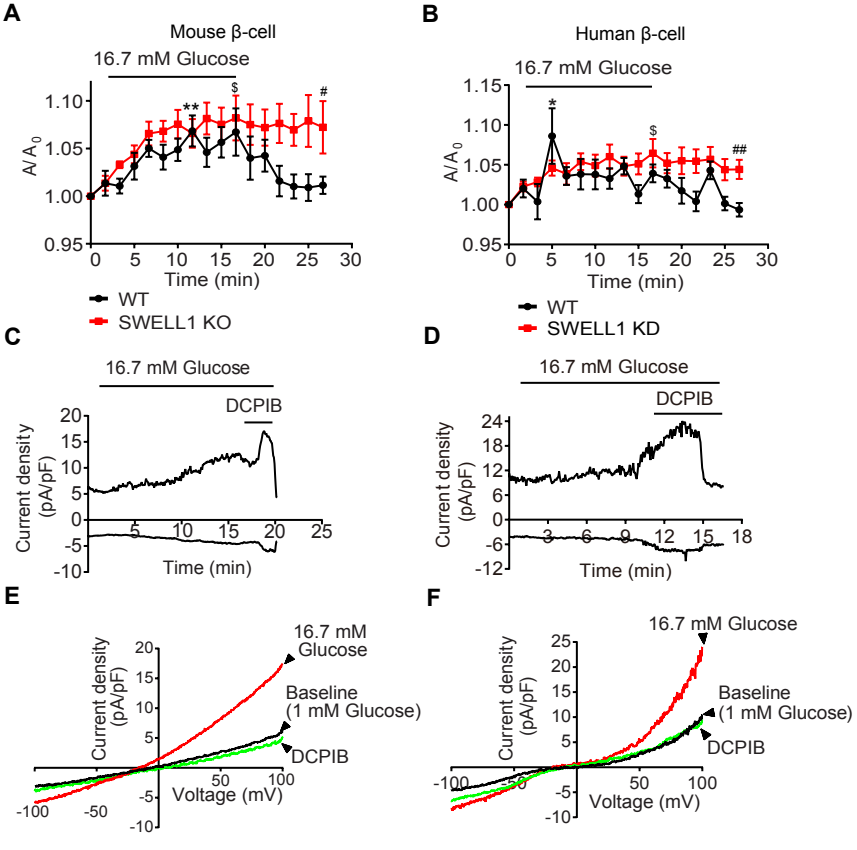
A
Mouse β-cell
16.7 mM Glucose
A/A0
Time (min)
WT
SWELL1 KO
B
Human β-cell
16.7 mM Glucose
A/A0
Time (min)
WT
SWELL1 KD
C
16.7 mM Glucose
DCPIB
Current density (pA/pF)
Time (min)
D
16.7 mM Glucose
DCPIB
Current density (pA/pF)
Time (min)
E
16.7 mM Glucose
Baseline (1 mM Glucose)
DCPIB
Current density (pA/pF)
Voltage (mV)
F
16.7 mM Glucose
Baseline (1 mM Glucose)
DCPIB
Current density (pA/pF)
Voltage (mV)

**Figure 3**

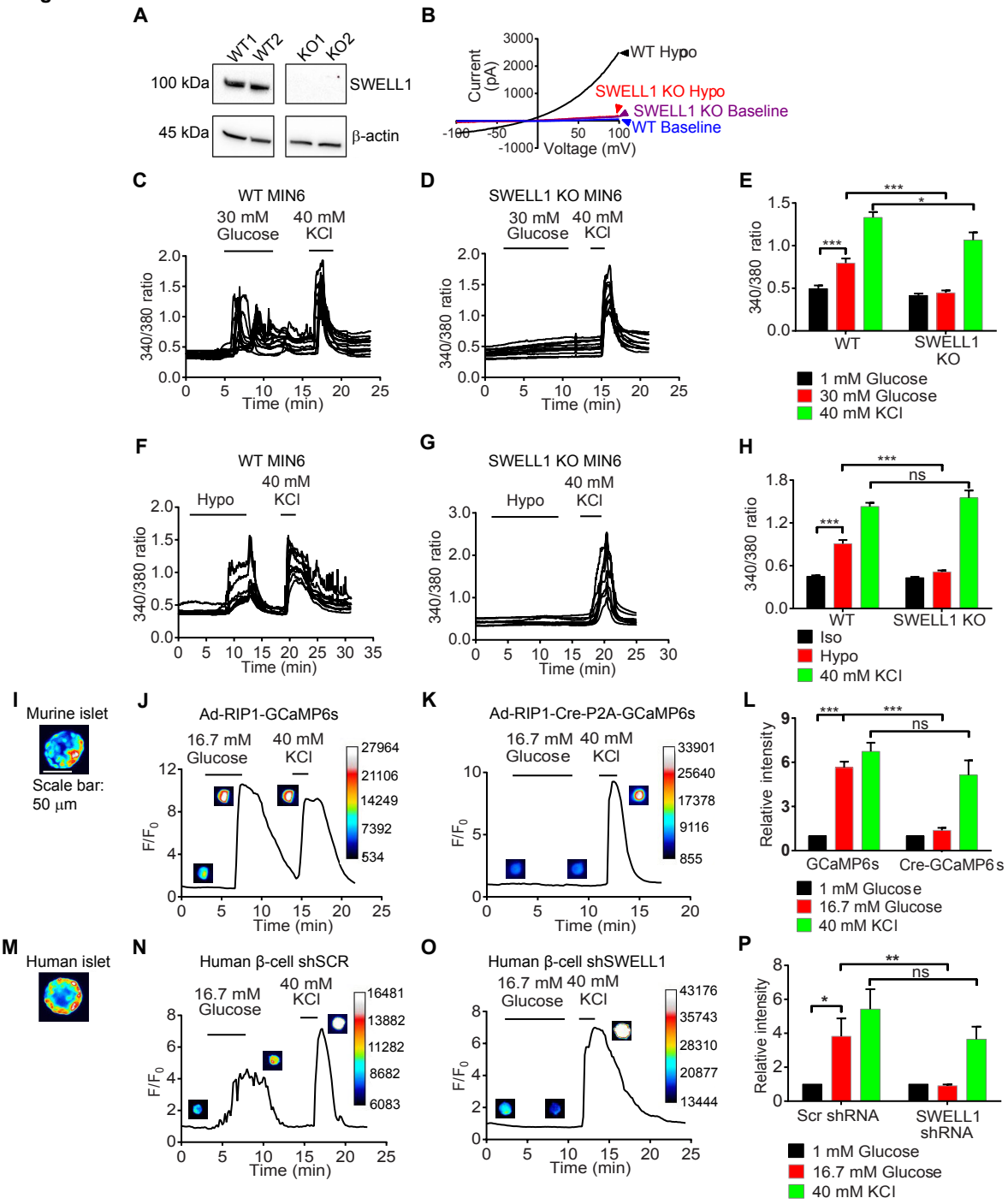
A
WT1
WT2
KO1
KO2
100 kDa
SWELL1
45 kDa
β-actin
B
Current (pA)
3000
2000
1000
-1000
-100
-50
50
100
Voltage (mV)
WT Hypo
SWELL1 KO Hypo
SWELL1 KO Baseline
WT Baseline
C
WT MIN6
30 mM Glucose
40 mM KCl
340/380 ratio
Time (min)
D
SWELL1 KO MIN6
30 mM Glucose
40 mM KCl
340/380 ratio
Time (min)
E
340/380 ratio
***
*
WT
SWELL1 KO
1 mM Glucose
30 mM Glucose
40 mM KCl
F
WT MIN6
Hypo
40 mM KCl
340/380 ratio
Time (min)
G
SWELL1 KO MIN6
Hypo
40 mM KCl
340/380 ratio
Time (min)
H
340/380 ratio
***
ns
WT
SWELL1 KO
Iso
Hypo
40 mM KCl
I
Murine islet
Scale bar: 50 μm
J
Ad-RIP1-GCaMP6s
16.7 mM Glucose
40 mM KCl
F/F0
27964
21106
14249
7392
534
Time (min)
K
Ad-RIP1-Cre-P2A-GCaMP6s
16.7 mM Glucose
40 mM KCl
F/F0
33901
25640
17378
9116
855
Time (min)
L
Relative intensity
***
***
ns
GCaMP6s
Cre-GCaMP6s
1 mM Glucose
16.7 mM Glucose
40 mM KCl
M
Human islet
N
Human β-cell shSCR
16.7 mM Glucose
40 mM KCl
F/F0
16481
13882
11282
8682
6083
Time (min)
O
Human β-cell shSWELL1
16.7 mM Glucose
40 mM KCl
F/F0
43176
35743
28310
20877
13444
Time (min)
P
Relative intensity
**
ns
*
Scr shRNA
SWELL1 shRNA
1 mM Glucose
16.7 mM Glucose
40 mM KCl

**Figure 4**

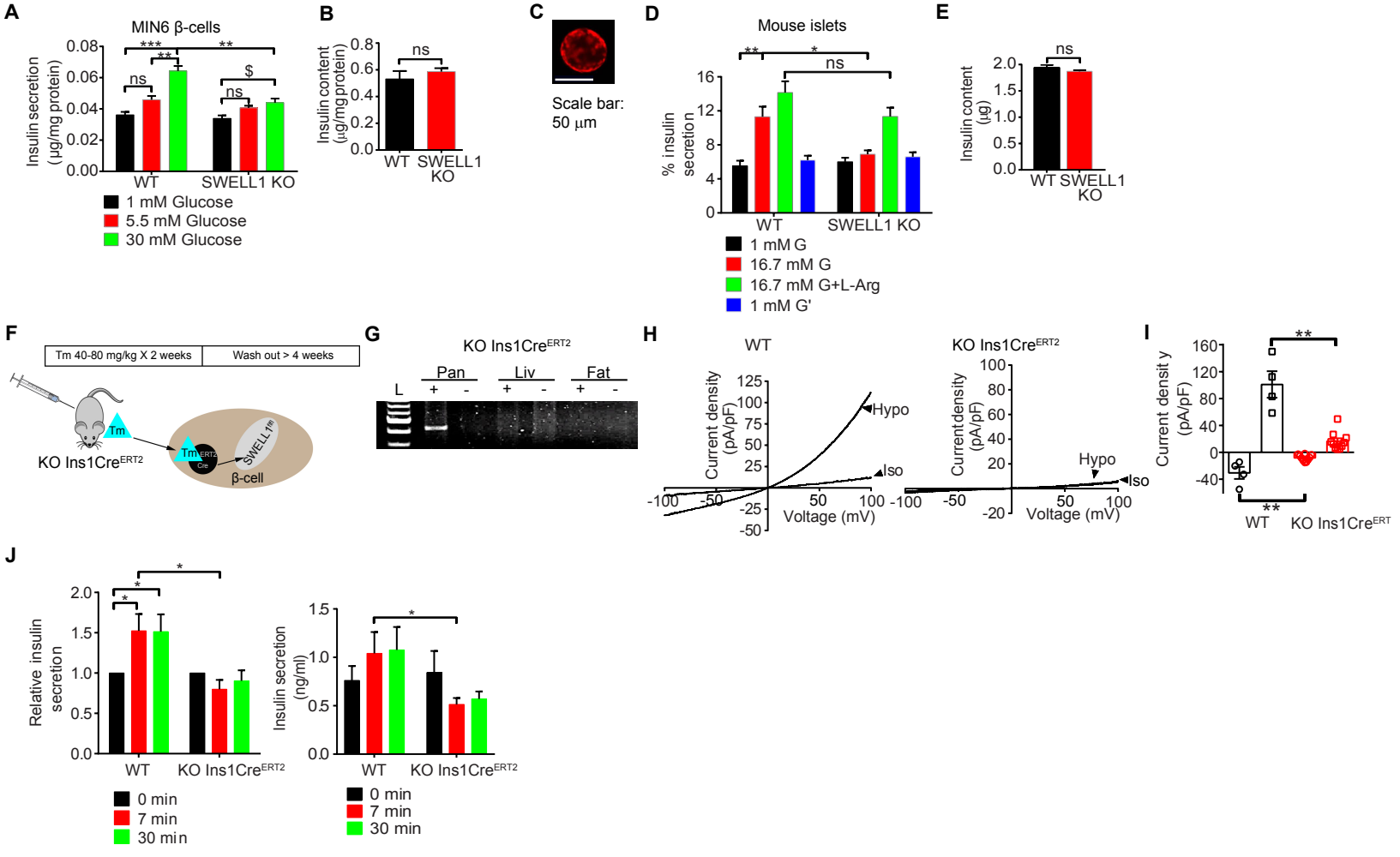
A
MIN6 β-cells
Insulin secretion (μg/mg protein)
0.08
0.06
0.04
0.02
0.00
***
**
**
ns
ns
$
WT
SWELL1 KO
1 mM Glucose
5.5 mM Glucose
30 mM Glucose
B
Insulin content (μg/mg protein)
0.8
0.6
0.4
0.2
0.0
ns
WT
SWELL1 KO
C
Scale bar: 50 μm
D
Mouse islets
% insulin secretion
16
12
8
4
0
**
*
ns
WT
SWELL1 KO
1 mM G
16.7 mM G
16.7 mM G+L-Arg
1 mM G'
E
Insulin content (μg)
2.0
1.5
1.0
0.5
0.0
ns
WT
SWELL1 KO
F
Tm 40-80 mg/kg X 2 weeks
Wash out > 4 weeks
Tm
KO Ins1Cre^ERT2
Tm^ERT2
Cre
SWELL1^fl/fl
β-cell
G
KO Ins1Cre^ERT2
Pan
Liv
Fat
L
+
-
+
-
+
-
H
WT
Current density (pA/pF)
125
100
75
50
25
-25
-50
-100
-50
50
100
Voltage (mV)
Hypo
Iso
KO Ins1Cre^ERT2
Current density (pA/pF)
100
80
60
40
20
-20
-50
50
100
Voltage (mV)
Hypo
Iso
I
Current density (pA/pF)
160
120
80
40
0
-40
**
**
WT
KO Ins1Cre^ERT
J
Relative insulin secretion
2.0
1.5
1.0
0.5
0.0
*
*
*
WT
KO Ins1Cre^ERT2
0 min
7 min
30 min
Insulin secretion (ng/ml)
1.5
1.0
0.5
0.0
*
WT
KO Ins1Cre^ERT2
0 min
7 min
30 min